Intergranular and Intragranular Precipitation on Continuous Cooling in Metastable β Ti-19Nb-2.5Fe-6Sn Alloy

Leticia F. Starck[a] (ID), *Maria Fernanda C. de Melo[a], Isabella C. Lancini[a], Marcio S.C. da Silva[a]* (ID),

João Felipe Q. Rodrigues[a] (ID), *Alessandra Cremasco[b]* (ID), *Rubens Caram[a]** (ID)

[a]Universidade de Campinas, Escola de Engenharia Mecânica, Campinas, SP, Brasil.
[b]Universidade de Campinas, Faculdade de Ciências Aplicadas, Limeira, SP, Brasil.

The Ti-19Nb-2.5Fe-6Sn alloy subjected to proper heat treatments is a promising material to be applied in orthopedic implants. This type of Ti alloy presents relatively low cost, good biocompatibility, and reasonable mechanical strength combined with low elastic modulus. In such an alloy, Fe improves mechanical strength while ω phase precipitation can be controlled by Sn addition. In this work, samples of the Ti-19Nb-2.5Fe-6Sn (wt.%) alloy were prepared by arc melting, hot swaging, and solution heat treatment. Results from the literature combined with thermodynamic simulations, differential scanning calorimetry (DSC), and heating/cooling experiments coupled with microstructural analyses were applied to determine the β transus temperature of this alloy. Following, the samples were solution heat treated in the β field and continuously cooled to room temperature at different rates. The effects of cooling rates on intergranular and intragranular α phase precipitation were evaluated. It was found that low cooling rates lead to intergranular precipitation while moderate cooling rates provide more expressive intragranular precipitation.

Keywords: *Titanium alloys, phase transformation, thermal analysis, thermodynamic simulations, heat treatment.*

1. Introduction

The application of titanium-based materials is quite diverse, ranging from jet engines to orthopedic implants, which is due to their unique properties like high tensile strengths, reduced elastic modulus, lightweight, high corrosion resistance, and good biocompatibility[1-3]. The Ti allotropy combined with proper alloying elements and suitable heat treatments opens the way to tailor the microstructure of Ti alloys and hence improve their properties[4]. In metastable β Ti alloys, a large variety of microstructures with stable and metastable phases can be produced, making necessary the understanding of their phase transformations[5,6]. Therefore, microstructure control based on selected processing pathways allows considerable improvements in mechanical behavior. The demand for high mechanical performance materials for load-bearing applications in the medical field has resulted in several new metastable β Ti alloys that are mainly based on the Nb, Ta e Zr elements[7-9]. Among them, two remarkable examples are the TNTZ (Ti-29Nb-13Ta-4.6Zr wt.%) and TNZT (Ti-35Nb-7Zr-5Ta wt.%) alloys, which are already employed in devices for orthopedic implantation[10,11]. In these alloys, Nb is the main β stabilizing element and its addition to Ti can contribute to β phase retention in metastable conditions, providing reduced elastic modulus coupled with improved biocompatibility and enhanced corrosion properties. The metastable β Ti alloys, after being solution heat treated at high temperatures, exhibit β phase retention

in rapidly cooled samples[8-10]. The resulting mechanical behavior is not suitable for structural applications, as they possess low mechanical strength. However, aging heat treatments lead to the controlled precipitation of α phase (HCP crystal structure) finely dispersed in a β phase matrix (BCC structure), improving strength. Depending on the alloy composition and aging heat treatment applied, the yield strength of metastable β Ti alloys can be improved up to 1200 MPa due to the fine-scale α phase precipitates[12-14].

It is known that α phase precipitate features, like morphology, size, and distribution, significantly affect the strengthening effect and hence, microstructure control based on selected processing pathways is of major importance[15-17]. On heating, α phase precipitation into β phase involves a complex process, which is usually assumed to be based on nucleation sites formed mainly by the nanometric isothermal ω phase[18-20]. An alternative path to obtain α phase precipitates into the β phase matrix comprises sample solution treatment above β transus temperature and then cooling it to intermediary temperature.

In such a case, α phase precipitation can occur heterogeneously from microstructural heterogeneities, such as second-phase precipitates or microstructural defects, like grain boundaries[21]. The α phase precipitation in grain boundaries is extremely deleterious to the mechanical properties, resulting in a significant reduction in ductility[22]. Intragranular precipitation, on the other hand, is very interesting as it can increase yield strength while maintaining moderate ductility[16]. Thus, it

*e-mail: caram@fem.unicamp.br

is an important challenge to establish ways to minimize intergranular precipitation in Ti alloys, as in the case of the Ti-Nb-Fe-Sn biomedical alloy. In such Ti alloys, Fe and Sn are alternatives to the high-cost Ta and Zr elements and their use resulted in Ti alloys with mechanical performance like those of TNTZ and TNZT alloys. Recent literature results suggest that the Fe addition to Ti-Nb alloys makes the β phase more stable and increases mechanical strength without substantially affecting the elastic properties[23,24]. Also, previous results indicate that Sn limits ω-phase precipitation in metastable β Ti alloys[25-27].

A composition that exhibits, depending on the processing route, reasonable yield strength combined with decreased elastic modulus is the Ti-19Nb-2.5Fe-6Sn (wt.%) alloy[28]. This composition, when β quenched results in a metastable microstructure formed by β and ω phases. When cooled at moderate cooling rates, it leads to α phase precipitates into the β phase matrix. Previous works have shown that different cooling rates can modify the α precipitation[29-31]. Chang et al.[29] showed the difference in the amount of α precipitated during continuous cooling with three different rates of a Ti–B19 alloy. The faster rate did not show α precipitation, the medium rate presented α precipitation predominantly in the grain boundaries (intergranular precipitation), and the slowest rate presented α in both intra and intergranular regions. Kherrouba et al.[30] showed that the high the cooling rate, the lower the β transus temperature, and the finer the α laths for Ti-6Al-4V. Campo et al.[31] studied the continuous cooling of the Ti-5553 alloy and noted finer α precipitates and more pronounced intragranular precipitation at higher cooling rates.

Therefore, this study attempts to investigate α phase precipitation in the newly developed Ti-19Nb-2.5Fe-6Sn alloy during continuous cooling. Firstly, the β transus temperature was identified by applying results from the literature combined with thermodynamic calculations and experimental measurements. Following, the samples were solution heat treated at temperatures above the β transus temperature, cooled at different rates, and then, the inter- and intragranular precipitation were assessed.

2. Experimental Procedure

Ingots of the Ti-19Nb-2.5Fe-6Sn alloy were prepared by arc melting in a furnace equipped with a water-cooled copper hearth and a non-consumable tungsten electrode under an argon atmosphere. These ingots were inverted and re-melted five times at each side, which means that the ingots were re-melted ten times, to obtain high chemical homogeneity. They were heat treated at 1000 ºC for 720 min under an inert atmosphere and rapidly cooled in water. Following, the ingots were hot-swaged at 1000 ºC to bars of 10 mm diameter bars and then, air-cooled. Disk-shaped samples of 3 mm thick were cut from these bars and then heat treated under different conditions. The samples' chemical composition was obtained using the X-ray fluorescence technique - XRF (Shimadzu EDX7000), while the interstitial content of O and N was measured using a Leco TC400 equipment.

Aiming to acquire information on the Ti-19Nb-2.5Fe-6Sn alloy β transus temperature, samples were investigated by differential scanning calorimetry (DSC), heating/cooling

experiments, and thermodynamic simulations. The DSC experiments were performed in a Netzsch STA 409 analyzer, using a sample weighing 50 mg, Al_2O_3 crucibles, and heating and cooling rates of 10 °C min^{-1}. To understand the phase transformation sequence, several DSC experiments were carried out. The thermodynamic simulations were performed by applying the ThermoCalc® software using the TCTI4 database.

To evaluate the α phase precipitation on cooling, three measurements were accomplished with different cooling rates. All tests consisted in heating different samples from room temperature to 1000 °C with a heating rate of 10 °C/min and remaining at this temperature for 30 minutes. Hence, only the β phase is obtained. Then, each sample was subjected to a different type of cooling procedure. The identification of each process and its steps can be found in Table 1. To determine the temperature evolution on cooling and hence, the cooling rate, a K-type thermocouple was inserted through a hole in the samples. To measure the cooling rates, at least two different samples were investigated. This thermocouple was connected to a computerized data acquisition system (Measuring Computer™).

Sample microstructure features were evaluated by employing standard metallographic procedures. After grinding and polishing, these samples were etched using a solution made up of 5 ml HF, 30 ml HNO_3 and 65 ml H_2O. Microstructures were investigated by scanning electron microscopy (SEM) using a Zeiss EVO equipped with an EDS apparatus. The microstructure analysis was also performed using the X-ray diffraction in a Panalytical X'Pert PRO diffractometer with Cu-Kα radiation (λ = 0.15406 nm) and applying 40 kV and 30 mA, a PIXcel detector and a spinner sample holder.

3. Results and Discussion

3.1. Chemical composition

The sample's measured chemical composition is presented in Table 2. The values presented are the average obtained

Table 1. Description of the cooling procedures.

Condition	Cooling Procedure
Furnace	Sample was furnace cooled under an Ar atmosphere
Quartz	Sample was air-cooled inside a quartz ampoule under an Ar atmosphere
Water quenched	Sample was water quenched

Table 2. Nominal and experimental contents obtained by X-ray fluorescence of the Ti-19Nb-2.5Fe-6Sn samples (wt.%).

Alloying element	Nominal	Measured
Ti	72.5	Balance
Nb	19	17.6 ± 1.0
Fe	2.5	2.7 ± 0.2
Sn	6	6.2 ± 0.7
O	-	0.06 ± 0.003
N	-	0.004 ± 0.0001

from three replicates. The interstitial contents are in good agreement with the ASTM-B-364-83 standard, as shown in Table 2. Hence, the values measured indicated that no substantial contamination occurred during sample preparation by arc melting. The Nb, Fe, and Sn contents were found to be very close to the nominal contents.

3.2. β-transus temperature

A key feature of a metastable β Ti alloy corresponds to its β transus temperature. The β transus temperature of the experimental Ti-19Nb-2.5Fe-6Sn alloy was assessed by four different methods: results from the literature, thermal analysis (DSC), thermodynamic simulations (ThermoCalc®), and heating and cooling experiments coupled with microstructure examination.

An initial approach to determine the Ti-19Nb-2.5Fe-6Sn alloy β transus temperature was based on the Ti-Nb phase diagram reported by Zhang et al.[32] and Bönisch et al.[33] combined with Yolton et al.[34] results. Figure 1 presents a partial stable and metastable Ti-Nb phase diagram calculated by Zhang et al.[32] and modified by Bönisch et al.[33]. If the Nb content is 19 wt.%, the corresponding β transus is near 727 °C, as shown in this diagram. The effects of Fe addition to the Ti-Nb were established by following the procedure described by Yolton et al.[34], which suggests that 1 wt.% Fe promotes a decrease in the β transus temperature of about 8.4 °C. In such a calculation, Sn is considered a neutral element and, consequently, its addition to Ti-Nb alloys does not cause any change in the β transus temperature. Then, the Ti-19Nb-2.5Fe-6Sn alloy β transus temperature was assumed, as a first attempt to be near 706 °C. However, according to Moraes et al.[35], the Sn addition, when combine with Nb, can act as β stabilizer, lowering the β transus temperature. Wang et al.[36] observed the same effect.

Figure 2 shows the one-axis diagram at the equilibrium condition of the Ti-19Nb-6Sn-2.5Fe alloy calculated with the real composition presented in Table 2, including oxygen and nitrogen. At equilibrium, the stability of an HCP structure rich in O, commonly denominated as α case, is noted at temperatures of about 900°C. The β-transus temperature is
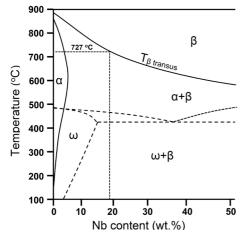
around 708°C, where, on colling, the β phase gives rise to α phase precipitation. Thus, the β phase becomes richer in Fe and Nb, while Sn tends to be segregated into the α phase. At about 500°C, the β phase tends to decompose into a disordered BCC phase rich in Nb (94% wt. Nb) and an ordered BCC phase related to TiFe intermetallic. Simultaneously, at that temperature, the α phase precipitation is intensified, being this phase rich in Sn.

Figure 3 shows the DSC heat flux evolution of the β quenched Ti-19Nb-2.5Fe-6Sn alloy. This experiment was carried out in an Al_2O_3 crucible, using a heating rate of 10 °C/min and under an Ar inert atmosphere. The results obtained were interpreted following Bönisch et al.[37] procedure. At the very beginning of heating, athermal ω phase dissolution took place, which corresponds to a weak endothermic peak between 100 and 200 °C. This phase dissolution is followed by isothermal ω phase precipitation between 220 and 420 °C.
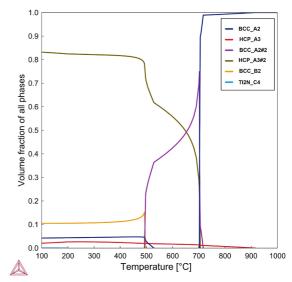

Figure 2. One-axis equilibrium diagram of Ti-19Nb-6Sn-2.5Fe alloy (ThermoCalc® software using the TCTI4 database).

Figure 1. The calculated partial stable and metastable Ti-Nb phase diagram showing the Ti-19Nb alloy β transus temperature[32].
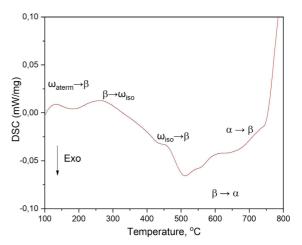

Figure 3. Evolution of heat flow (DSC) during the heating cycle of an ST/WQ sample of Ti-19Nb-2.5Fe-6Sn alloy.

Between 440 °C and 480 °C, it seems that the isothermal ω phase dissolution occurred. The α phase precipitation starts at around 500 °C and as the temperature increases, α phase is replaced with β phase. At around 745 °C, a clear change in the slope of the heat flow evolution is detected, but it cannot be directly related to the β-transus temperature. This result suggested that the Ti-19Nb-2.5Fe-6Sn alloy β transus temperature is below 745 °C.

The Ti-19Nb-2.5Fe-6Sn alloy β transus temperature was also assessed using metallographic procedures. An interactive procedure was carried out in which the samples were annealed at a certain temperature, rapidly quenched and their microstructure was examined by X-ray diffraction and microscopy. The samples were solution heat treated at 1000 °C for 1 h, cooled to 850 °C (Figure 4a), isothermally treated at this temperature for 30 min and water quenched. The α phase precipitation was investigated and the findings

have indicated that the resulting microstructure, as expected, was made up of β phase only.

A similar procedure was applied to a new sample, but the isothermal heat treatment temperature was dropped to 750 °C (Figure 4b). The results indicated that this temperature was again above the β transus temperature since the microstructure consisted of β phase only. Next, another sample was heat treated at 700 °C (Figure 4c), held at this temperature for 30 min, and rapidly quenched. The corresponding microstructure and X-ray diffraction pattern revealed α phase precipitates, implying that the β transus temperature was still above the selected temperature, i.e., between 700 °C and 750 °C. Following, samples were heat treated at 730 °C (Figure 4d) and 740 °C (Figure 4e), and the microstructure analyses exposed α phase precipitation, Finally, the last temperature applied was 745 °C (Figure 4f), which revealed again α phase precipitation. This information
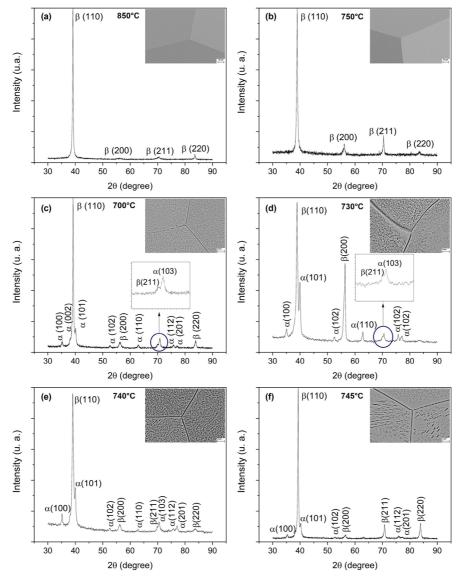

Figure 4. X-ray diffraction patterns of quenched samples from different temperatures.

led to the conclusion that the β transus temperature is between 745 °C and 750 °C. If these results are compared with results obtained from thermodynamic simulations and results obtained by Yolton et al.[34], a difference near 40 °C is observed and it may be caused by the assumption that Sn is a neutral element. Another possible explanation for such a difference is related to the oxygen content, which could forward the β transus temperature to higher temperatures. Oxygen is known to be a powerful α stabilizer element. Table 3 summarizes the beta transus temperature for each analyzed method.
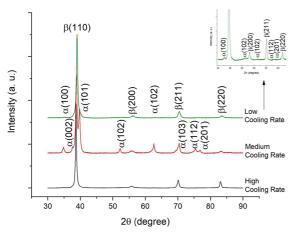
3.3. Effects of cooling rate on α-phase precipitation

After solution heat treatment in the β field, three samples were subjected to different cooling procedures, resulting in different cooling rates. The data acquisition allowed to calculate the corresponding cooling rate by using the angular coefficient of the temperature *versus* time curves. The resulting cooling rates are depicted in Table 4.

The microstructures after the different cooling procedures were investigated by X-ray diffraction measurements and the corresponding patterns are shown in Figure 5.

According to the X-ray diffraction patterns, the samples subjected to the WQ condition (high cooling rate) resulted in β phase only, while the other routes led to some α phase precipitation. These findings show that the low and medium cooling rates applied to the samples were sufficiently low to avoid a full metastable microstructure, leading to a stable α phase formation on cooling. The phase volume fractions for these two conditions could not be directly related to the diffraction peak intensities due to the samples' crystallographic texture.

The SEM images of samples subjected to the different cooling conditions are also shown in Figure 6. The microstructure cooled

Figure 5. X-ray diffraction patterns of samples processed under different cooling rates.

Table 3. Beta-transus temperature for each analyzes method.

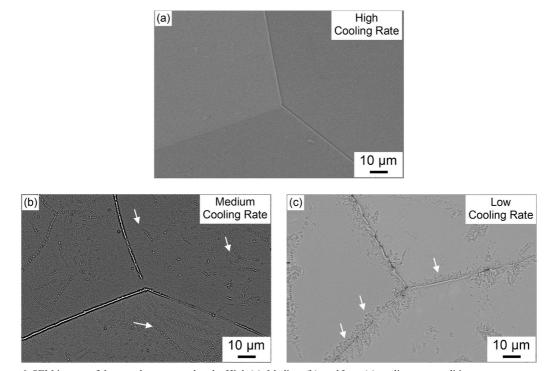| Method	Beta-transus temperature (°C)
Literature	706
ThermoCalc® simulations	708
DSC	>745
Isothermal heat treatment	745

Figure 6. SEM images of the samples processed under High (a), Medium (b), and Low (c) cooling rate conditions.

Table 4. Cooling rates for the five cooling conditions.

Condition	Cooling rate (°C/min)
Furnace	3.4 (low)
Quartz	265 (medium)
WQ	>1000 (high)

at a high cooling rate is formed by β phase only, as detected by the corresponding X-ray diffraction pattern. The α phase was detected in samples cooled at medium and low rates and some morphologic differences were detected. The samples processed at medium rates show smaller and more dispersed precipitates than the ones obtained at low rates. The medium-cooled rate microstructure also showed more intense intragranular precipitation when compared to the low-cooling rate procedure. According to Campo et al.[31], in a continuous cooling process, the higher the cooling rate, the more intense the intragranular precipitation portion is when compared to the intergranular precipitation.

4. Conclusions

In summary, the Ti-19Nb-2.5Fe-6Sn alloy β transus temperature was investigated using different approaches. According to Yolton et al.[34], this temperature was calculated to be near 706 °C. Using (DSC) results, this β transus temperature was detected to be below 745 °C. Thermodynamic simulations suggested that the β transus temperature is around 708°C, while metallographic procedures indicated that the Ti-19Nb-2.5Fe-6Sn alloy β transus temperature is near 745 °C. Temperature differences are probably related to the oxygen content, which could forward the β transus temperature to higher temperatures. Sn addition to the Ti-Nb alloys can also change the β transus temperature. Samples subjected to high cooling rate resulted in metastable β phase only, while low and medium cooling rates were sufficiently low to avoid a full metastable microstructure, leading to partial precipitation of stable α phase on cooling. Results also confirmed that the higher the cooling rate, the more intense the intragranular precipitation portion compared to the intergranular precipitation.

5. Acknowledgements

6. References

1. Lütjering G, Williams JC. Titanium. 2nd ed. Cambridge: Springer; 2007.

2. Banerjee D, Williams JC. Perspectives on titanium science and technology. Acta Mater. 2013;61:844-79.

3. Banerjee S, Mukhopadhyay P. Phase transformations: examples from titanium and zirconium alloys. Amsterdam: Elsevier; 2007.

4. Leyens C, Peters M, editors. Titanium and titanium alloys: fundamentals and applications. Weinheim: Wiley-VCH Verlag; 2003.

5. Zheng Y, Williams REA, Fraser HL. Characterization of a previously unidentified ordered orthorhombic metastable phase in Ti-5Al-5Mo-5V-3Cr. Scr Mater. 2016;113:202-5.

6. Zheng Y, Williams REA, Sosa JM, Alam T, Wang Y, Banerjee R et al. The indirect influence of the ω phase on the degree of refinement of distributions of the α phase in metastable β-Titanium alloys. Acta Mater. 2016;103:165-73. http://dx.doi.org/10.1016/j.actamat.2015.09.053.

7. Tang X, Ahmed T, Rack HJ. Phase transformations in Ti-Nb-Ta and Ti-Nb-Ta-Zr alloys. J Mater Sci. 2000;35:1805-11. http://dx.doi.org/10.1023/A:1004792922155.

8. Geetha M, Singh AK, Asokamani R, Gogia AK. Ti based biomaterials, the ultimate choice for orthopaedic implants - a review. Prog Mater Sci. 2009;54:397-425.

9. Niinomi M, Nakai M. Titanium-based biomaterials for preventing stress shielding between implant devices and bone. Int J Biomater. 2011;2011:836587.

10. Kuroda D, Niinomi M, Morinaga M, Kato Y, Yashiro T. Design and mechanical properties of new β type titanium alloys for implant materials. Mater Sci Eng A. 1998;243:244-9. http://dx.doi.org/10.1016/S0921-5093(97)00808-3.

11. Long M, Rack HJ. Titanium alloys in total joint replacement-a materials science perspective. Biomaterials. 1998;19(18):1621-39.

12. Nag S, Banerjee R, Srinivasan R, Hwang JY, Harper M, Fraser HL. ω-Assisted nucleation and growth of α precipitates in the Ti–5Al–5Mo–5V–3Cr–0.5Fe β titanium alloy. Acta Mater. 2009;57:2136-47. http://dx.doi.org/10.1016/j.actamat.2009.01.007.

13. Boyer RR, Briggs RD. The use of β titanium alloys in the aerospace industry. J Mater Eng Perform. 2013;22:2916-20.

14. Cotton JD, Briggs RD, Boyer RR, Tamirisakandala S, Russo P, Shchetnikov N et al. State of the art in beta titanium alloys for airframe applications. JOM. 2015;67:1281-303.

15. Lütjering G. Influence of processing on microstructure and mechanical properties of (α + β) titanium alloys. Mater Sci Eng A. 1998;243(1-2):32-45.

16. Ivasishin OM, Markovsky PE, Matviychuk YV, Semiatin SL, Ward CH, Fox S. A comparative study of the mechanical properties of high-strength β-titanium alloys. J Alloys Compd. 2008;457:296-309. http://dx.doi.org/10.1016/j.jallcom.2007.03.070.

17. Du Z, Xiao S, Xu L, Tian J, Kong F, Chen Y. Effect of heat treatment on microstructure and mechanical properties of a new β high strength titanium alloy. Mater Des. 2014;55:183-90. http://dx.doi.org/10.1016/j.matdes.2013.09.070.

18. Li T, Kent D, Sha G, Stephenson LT, Ceguerra AV, Ringer SP et al. New insights into the phase transformations to isothermal ω and ω-assisted α in near β-Ti alloys. Acta Mater. 2016;106:353-66. http://dx.doi.org/10.1016/j.actamat.2015.12.046.

19. Zheng Y, Williams REA, Wang D, Shi R, Nag S, Kami P et al. Role of ω phase in the formation of extremely refined intragranular α precipitates in metastable β-titanium alloys. Acta Mater. 2016;103:850-8. http://dx.doi.org/10.1016/j.actamat.2015.11.020.

20. Guo Y, Wei S, Yang S, Ke Y, Zhang X, Zhou K. Precipitation behavior of ω phase and ω→α transformation in near β Ti-5Al-5Mo-5V-1Cr-1Fe alloy during aging process. Metals. 2021;11:1-11. http://dx.doi.org/10.3390/met11020273.

21. Nag S, Banerjee R, Fraser HL. Intra-granular alpha precipitation in Ti–Nb–Zr–Ta biomedical alloys. J Mater Sci. 2009;44:808-15. http://dx.doi.org/10.1007/s10853-008-3148-2.

22. Chiu E, Srivastava A. Intergranular ductile failure of materials with plastically heterogeneous grains. Materialia. 2022;23:101439. http://dx.doi.org/10.1016/j.mtla.2022.101439.

23. Costa FH, Salvador CAF, Mello MG, Caram R. Alpha phase precipitation in Ti-30Nb-1Fe alloys - phase transformations in continuous heating and aging heat treatments. Mater Sci Eng A. 2016;677:222-9. http://dx.doi.org/10.1016/j.msea.2016.09.023.

24. Lopes ÉSN, Salvador CAF, Andrade DR, Cremasco A, Campo KN, Caram R. Microstructure, mechanical properties, and electrochemical behavior of Ti-Nb-Fe alloys applied as biomaterials. Metall Mater Trans, A Phys Metall Mater Sci. 2016;47:3213-26. http://dx.doi.org/10.1007/s11661-016-3411-0.

25. Moraes PEL, Contieri RJ, Lopes ESN, Robin A, Caram R. Effects of Sn addition on the microstructure, mechanical properties and corrosion behavior of Ti-Nb-Sn alloys. Mater Charact. 2014;96:273-81. http://dx.doi.org/10.1016/j.matchar.2014.08.014.

26. Lopes ÉSN, Cremasco A, Contieri RJ, Caram R. Effects of aging heat treatment on the microstructure of Ti-Nb and Ti-Nb-Sn alloys employed as biomaterials. Adv Mat Res. 2011;324:61-4.

27. Mello MG, Salvador CAF, Cremasco A, Caram R. The effect of Sn addition on phase stability and phase evolution during aging heat treatment in Ti-Mo alloys employed as biomaterials. Mater Charact. 2015;110:5-13. http://dx.doi.org/10.1016/j.matchar.2015.10.005.

28. Dal Bó MR, Salvador CAF, Mello MG, Lima DD, Faria GA, Ramirez AJ et al. The effect of Zr and Sn additions on the microstructure of Ti-Nb-Fe gum metals with high elastic admissible strain. Mater Des. 2018;160:1186-95. http://dx.doi.org/10.1016/j.matdes.2018.10.040.

29. Chang H, Gautier EA, Zhou L. Phase transformation kinetics in metastable titanium alloys. Chin Sci Bull. 2014;59:1773-7. http://dx.doi.org/10.1007/s11434-014-0210-0.

30. Kherrouba N, Bouabdallah M, Badji R, Carron D, Amir M. Beta to alpha transformation kinetics and microstructure of Ti-6Al-4V alloy during continuous cooling. Mater Chem Phys. 2016;181:462-9. http://dx.doi.org/10.1016/j.matchemphys.2016.06.082.

31. Campo KN, Fanton L, Mello MG, Moon SC, Dippenaar R, Caram R. Exploring the Ti-5553 phase transformations utilizing in-situ high-temperature laser-scanning confocal microscopy. Mater Charact. 2020;159:110013. http://dx.doi.org/10.1016/j.matchar.2019.110013.

32. Zhang Y, Liu H, Jin Z. Thermodynamic assessment of the Nb-Ti system. Calphad. 2001;25:305-17. http://dx.doi.org/10.1016/S0364-5916(01)00051-7.

33. Bönisch M, Panigrahi A, Calin M, Waitz T, Zehetbauer M, Skrotzki W et al. Thermal stability and latent heat of Nb–rich martensitic Ti-Nb alloys. J Alloys Compd. 2017;697:300-9. http://dx.doi.org/10.1016/j.jallcom.2016.12.108.

34. Yolton CF, Froes FH, Malone RF. Alloying element effects in metastable beta titanium alloys. Metall Trans, A, Phys Metall Mater Sci. 1979;10:132-4. http://dx.doi.org/10.1007/BF02686421.

35. Moraes PEL, Contieri RJ, Lopes ESN, Robin A, Caram R. Effects of Sn addition on the microstructure, mechanical properties and corrosion behavior of Ti-Nb-Sn alloys. Mater Charact. 2014;96:273-81. http://dx.doi.org/10.1016/j.matchar.2014.08.014.

36. Wang BL, Zheng YF, Zhao LC. Effects of Sn content on the microstructure, phase constitution and shape memory effect of Ti-Nb-Sn alloys. Mater Sci Eng A. 2008;486:146-51. http://dx.doi.org/10.1016/j.msea.2007.08.073.

37. Bönisch M, Calin M, Waitz T, Panigrahi A, Zehetbauer M, Gebert A et al. Thermal stability and phase transformations of martensitic Ti-Nb alloys. Sci Technol Adv Mater. 2013;14(5):055004. http://dx.doi.org/10.1088/1468-6996/14/5/055004.